Physics and Astronomy Publications

Physics and Astronomy

2-11-2011

Magnetization distribution in the tetragonal Ba(Fe1-xCox)(2)As-2, x=0.066 probed by polarized neutron diffraction

K. Prokeš
Helmholtz-Zentrum Berlin für Materialien und Energy

A. Gukasov
Laboratoire Léon Brillouin CEA-Saclay

D. N. Argyriou
Helmholtz-Zentrum Berlin für Materialien und Energy

Sergey L. Bud'ko
Iowa State University and Ames Laboratory, budko@ameslab.gov

Paul C. Canfield
Iowa State University and Ames Laboratory, canfield@ameslab.gov

See next page for additional authors

Magnetization distribution in the tetragonal Ba(Fe1-xCox)(2)As-2, x=0.066 probed by polarized neutron diffraction

Abstract

Polarized neutron diffraction has been performed on a tetragonal Ba(Fe1-xCox)(2)As-2, x=0.066 single crystal under an applied magnetic field of 6 T directed along the [(1) over bar 10] direction to determine the magnetic structure factors of various Bragg reflections. The maximum entropy reconstruction based on bulk magnetization measurements and polarized neutron diffraction data reveal a small induced magnetic moment residing on the 4d Wyckoff site that is occupied by Fe/Co atoms. No significant magnetization density has been found on the Ba and As atomic positions. The small polarizability of Fe/Co sites leads to flipping ratios very close to 1.00. Our data suggest a non-zero orbital contribution to the Fe/Co magnetic form factor in good agreement with recent theoretical and experimental studies.

Disciplines

Condensed Matter Physics

Comments

Authors

K. Prokeš, A. Gukasov, D. N. Argyriou, Sergey L. Bud'ko, Paul C. Canfield, Andreas Kreyssig, and Alan I. Goldman

Magnetization distribution in the tetragonal Ba(Fe$_{1-x}$Co$_x$)$_2$As$_2$, x=0.066 probed by polarized neutron diffraction

View the article online for updates and enhancements.

Magnetization distribution in the tetragonal Ba(Fe$_{1-x}$Co$_x$)$_2$As$_2$, x = 0.066 probed by polarized neutron diffraction

K. Prokeš[1(a)], A. Gukasov[2], D. N. Argyriou[1], S. L. Bud'ko[3,4], P. C. Canfield[3,4], A. Kreyssig[3,4] and A. I. Goldman[3,4]

[1] *Helmholtz-Zentrum Berlin für Materialien und Energy - Hahn-Meitner-Platz 1, 14109 Berlin, Germany, EU*
[2] *Laboratoire Léon Brillouin CEA-Saclay - Gif-sur-Yvette 91191, France, EU*
[3] *Ames Laboratory, U.S. DOE, Iowa State University - Ames, IA 50011, USA*
[4] *Department of Physics and Astronomy, Iowa State University - Ames, IA 50011, USA*

Abstract – Polarized neutron diffraction has been performed on a tetragonal Ba(Fe$_{1-x}$Co$_x$)$_2$As$_2$, $x = 0.066$ single crystal under an applied magnetic field of 6 T directed along the [$\bar{1}$10] direction to determine the magnetic structure factors of various Bragg reflections. The maximum entropy reconstruction based on bulk magnetization measurements and polarized neutron diffraction data reveal a small induced magnetic moment residing on the 4d Wyckoff site that is occupied by Fe/Co atoms. No significant magnetization density has been found on the Ba and As atomic positions. The small polarizability of Fe/Co sites leads to flipping ratios very close to 1.00. Our data suggest a non-zero orbital contribution to the Fe/Co magnetic form factor in good agreement with recent theoretical and experimental studies.

Introduction. – Since the discovery of the so-called 1111 oxypnictide [1] and 112 iron arsenide [2] superconducting families of compounds, an extensive experimental effort has been devoted to determine their basic physical properties and the relationships between structure, magnetism, composition and superconductivity (SC) [3,4]. Both classes of compounds adopt a layered crystal structure consisting of Fe-As layers separated by the either oxide blocks or alkaline-earth (AE) atoms, respectively. The parent compounds are metallic in contrast to cuprates. SC state can occur at temperatures as high as $T_c = 57.4$ K either upon electron or hole doping or underpressure [5–8]. At least in the case of CaFe$_2$As$_2$ it was demonstrated that uniaxial pressure also leads to SC state (albeit with lower T_c) [9]. The doping and/or pressure suppress also a tetragonal to orthorhombic distortion and antiferromagnetic (AF) order. As the structural and AF order are suppressed, SC emerges, although there are now several examples of microscopic coexistence between these states [6,10–12].

Theoretical *ab initio* calculations studies have revealed a strong hybridization between electronic states residing at Fe and As sites [13–15]. Indeed, it has been argued that Fe-As electron states play a significant role in the SC properties of iron arsenides. However, extensive studies of the phonon spectra suggest that, unlike the cuprates, electron-phonon interactions are not responsible for SC in iron pnictides. Recent inelastic neutron scattering experiment on optimally doped 122 compounds revealed an existence of a resonant spin excitation [16,17], which seems to be a unifying feature for iron pnictides despite different details in the crystal and magnetic structure [18]. Since neutron experiments show that the AF order is of a spin-density wave type of Fe moments and the SC appears just at the verge of the long-range AF order, it is natural to assume that spin fluctuations are involved in the formation of SC. Furthermore, the potential involvement of orbital components and their modifications at T_N as suggested by angle-resolved photoemission spectroscopy (ARPES) [19,20] is highly debated. Several studies have tried to identify whether orbital order plays any significant role in the magnetism or SC of these compounds.

(a)E-mail: prokes@helmholtz-berlin.de

However, the number of such experiments is still rather limited, due to experimental difficulties connected with very small magnetic susceptibility, existence of the orthorhombic distortion below the T_{TO}, AF order below T_N and Meissner effect below T_c that obscures the data significantly. For all of the reasons discussed above, it is important to characterize and understand the microscopic details of magnetism in the oxypnictide parent compounds and superconductors.

In order to determine which electronic states giving rise to spin fluctuations in the paramagnetic state and whether orbital part is involved, an attempt to determine the density map in magnetic fields have been performed. The polarized neutron diffraction (PND) technique is an extremely powerful tool as it gives direct information on the distribution of the magnetization in the unit cell and allows for the identification of the spin and orbital parts of the magnetic moments [21]. To tackle this problem, a Ba(Fe$_{1-x}$Co$_x$)$_2$As$_2$, $x = 0.066$ single crystal of good quality, that does not exhibit the structural distortion down to the lowest temperatures and is superconducting below $T_c = 24$ K has been selected.

Experimental. – A single crystal with a mass of 88 mg used in the present study was grown from Fe-As self-flux using conventional high-temperature solution growth [22]. It has been checked for its crystallinity by the X-ray Laue back scattering technique and the composition was measured at several different positions using wavelength dispersive spectroscopy (WDS). The combined statistical and systematic error on the Co composition is not greater than 5%. DC magnetic susceptibility and magnetization curves were measured on the same sample used for the PND experiment using the SQUID magnetometer (Quantum Design) in fields up to 6 T applied along the [$\bar{1}$10] direction.

In a neutron diffraction experiment on a paramagnet with field-induced magnetic moments one typically determines the magnetic structure factor $F_M(\mathbf{Q}) \propto \sum_j \mu_{j\perp} f_j(\mathbf{Q}) e^{i\mathbf{Q}\cdot\mathbf{r}_j}$, where $\mu_{j\perp}$ is the component of the j-th magnetic moment perpendicular to the scattering vector $\mathbf{Q}$ and $f_j(\mathbf{Q})$ is the magnetic form factor of the j-th ion at position r_j in the unit cell [23]. Using unpolarized neutrons one records an intensity proportional to the sum of $|F_M(\mathbf{Q})|^2$ and the nuclear structure factor squared $|F_N(\mathbf{Q})|^2 \propto |\sum_j b_j e^{i\mathbf{Q}\cdot\mathbf{r_j}}|^2$. However, when the magnetic moment is small, as in the present case, $|F_M(\mathbf{Q})|^2$ is too small as compared to $|F_N(\mathbf{Q})|^2$ and cannot be determined precisely. One way to improve the sensitivity is the use of polarized neutrons [21]. In the PND experiment one then measures the intensities $I^{\pm}(\mathbf{Q}) \propto |F_N(\mathbf{Q}) \pm F_M(\mathbf{Q})|^2$, where the $+$ and $-$ sign refer to up and down polarization directions of the incoming neutron beam. In practise one collects flipping ratios $R(\mathbf{Q}) = I^+(\mathbf{Q})/I^-(\mathbf{Q})$ at many Bragg reflections.

The PND experiment was carried out at the 5c1 and 6t2 diffractometers [24] installed at the ORPHÈE 14 MW
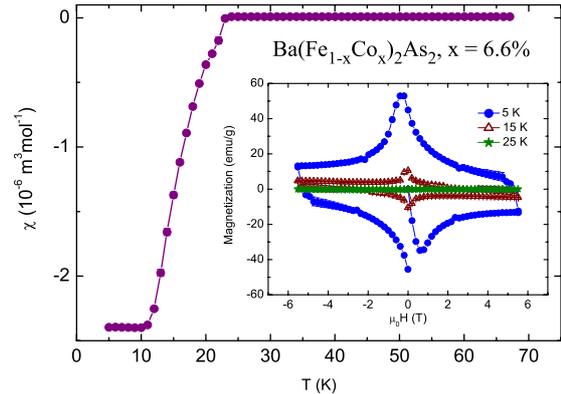

Fig. 1: (Color online) Temperature dependence of the molar magnetic susceptibility of Ba(Fe$_{1-x}$Co$_x$)$_2$As$_2$, $x = 0.066$ single crystal measured on a zero-field–cooled sample in a field of 1 T applied along the [$\bar{1}$10] direction. In the inset the magnetization loops measured on a zero-field–cooled sample at 5, 15 and 25 K are shown.

reactor of the Lèon Brillouin Laboratory, CEA/CNRS Saclay with the neutron beam polarized to 91% and 97%, respectively. The single crystal was attached to the cold finger of the cryomagnet with the [110] axis vertical, along the applied magnetic field of 6T. At the 5c1 instrument, two data sets $R(\mathbf{Q})$ were collected with the incident wavelength λ of 0.8495 Å at 2 K and 25 K. Each data set consisted of 25 inequivalent reflections $\sin\theta/\lambda < 0.65$. At 6t2 only one, set of data at 25 K was collected with an incident wavelength of $\lambda = 1.40$ Å.

For an accurate interpretation of the PND data the crystal structure has to be well known. This is usually determined using conventional unpolarized neutron diffraction experiment leading to a precise knowledge of $F_N(\mathbf{Q})$.

To refine the As atomic position, the only free positional parameter in the structure, and other structure parameters that include the distribution of Fe/Co atoms and extinction parameter for our crystal, integrated intensities of nuclear reflections were collected on the E2 and E4 diffractometers installed at Helmholtz Zentrum Berlin. The incident wavelength used at both instruments was 2.44 Å. In this case the crystal was mounted inside an orange cryostat in two different orientations: with its c-axis along and perpendicular to the rotational axis. In the course of refinement we have restricted ourselves to the use of isotropic temperature factors. The extinction correction was found to be negligible. The refined positional parameter z for As of 0.3541(3) is very similar to the literature value [25]. The occupation of Co/Fe was found to be statistical with stoichiometry identical within the error bars to the nominal 6.6%.

Results. – In fig. 1 the temperature dependence of the DC magnetic susceptibility of Ba(Fe$_{1-x}$Co$_x$)$_2$As$_2$, $x = 0.066$ is shown. Clearly, the SC appears below $T_c = 24$ K. In the inset of fig. 1 we show the field dependence of the magnetization measured at 5, 15 and 25 K after
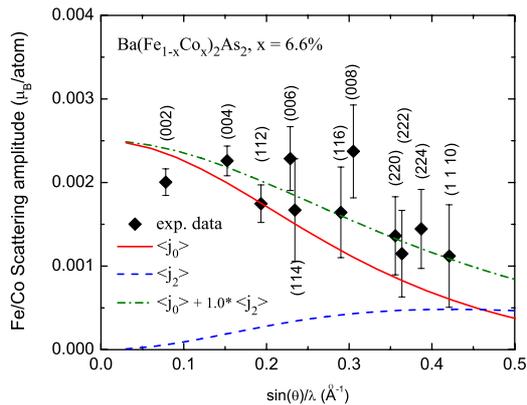
Fig. 2: (Color online) Experimental magnetic form factor of Ba(Fe$_{1-x}$Co$_x$)$_2$As$_2$, $x = 0.066$ determined in a field of 6 T applied along the $[\bar{1}10]$ direction at 25 K (points). The solid line shows the $\langle j_0 \rangle$ part of the theoretical magnetic form factor calculated for statistically distributed Fe^{2+}/Co^{2+} in a ratio corresponding to the stoichiometry of Ba(Fe$_{1-x}$Co$_x$)$_2$As$_2$, $x = 0.066$ normalized to the bulk magnetization. The dashed line represents the $\langle j_2 \rangle$ part and the dot-dashed line the sum of both.

zero-field cooling. The magnetization measured above the superconducting phase transition at 25 K that is needed to extract the magnetic moment per Fe/Co site consists of two contributions. Apart from the field-induced paramagnetic part originating from states near the Fermi energy, there is a diamagnetic component that is present in all materials. In the majority of cases, the latter can be neglected as it is usually much smaller than the former contribution. However, in our case it needs to be taken into account. It appeared that after accounting for the diamagnetic contribution we can estimate the field-induced magnetization at 25 K and 6 T to be $\approx 0.0050(4)$ μ_B/f.u.

Since the magnetic susceptibility of Ba(Fe$_{1-x}$Co$_x$)$_2$As$_2$, $x = 0.066$ and the magnetic moment induced at 6 T is small, the measured flipping ratios are all close to 1.00. To reduce the statistical error we collected data for several hours each and repeated the measurement a few times. The flipping ratios of equivalent reflections were averaged and used in the determination of $F_M(\mathbf{Q})$'s and further analysis. The resulting 16 observations were analyzed by two different methods: i) comparing the data with a model expression for the Fe/Co magnetic form factor and ii) by constructing magnetization density maps produced by the maximum entropy technique (MAXENT) [26].

The experimentally determined magnetic form factor calculated from the observed $R(\mathbf{Q})$'s by assuming a magnetic moment on the Fe/Co positions only and normalized to the magnetic moment determined from the magnetic bulk measurement, is shown in fig. 2. The spin ($\langle j_0 \rangle$) and orbital ($\langle j_i \rangle$, $i = 2, 4, \ldots$) contributions to the magnetic form factor for various atoms was tabulated by Freeman and Watson [27]. For our work we have utilized

the weighted average of Fe^{2+} and Co^{2+} magnetic form factors. At low $\sin\theta/\lambda$, we obtained, within given error bars, a satisfactory description of the data by assuming only a spin contribution, *i.e.* limiting ourselves to $\langle j_0 \rangle$ and normalizing at $\mathbf{Q} = 0$ to a value obtained from the magnetization measurements. The only exception is the (002) reflection that is clearly below the magnetic form factor curve. A possible explanation would be, for instance, slightly overestimated magnetic moment per Fe/Co site from magnetic bulk measurements. Although at higher θ/λ value, some deviations become apparent, signaling some asphericity of the magnetization distribution and the need to also include an orbital contribution, we were not able to determine the relative contributions from different orbitals precisely. Nevertheless, we include in fig. 2 the magnetic form factor calculated for the statistical distribution of Fe^{2+}/Co^{2+} in the form $\langle j_0 \rangle + 1.0 * \langle j_2 \rangle$ that gives a reasonable agreement in the whole θ/λ range. One should, however, note that if one treats the magnetic moment per Fe/Co site as a free parameter leading to $0.0044(2)$ μ_B/f.u. as compared to $0.0050(4)$ μ_B/f.u. determined from SQUID magnetometer, one arrives to expression $\langle j_0 \rangle + 2.1 * \langle j_2 \rangle$ and a better agreement with experimental data (including the (002) reflection).

Application of MAXENT gives the most probable magnetization distribution map compatible with the measured structure factors and their experimental uncertainties. Compared to the usual Fourier synthesis it does not require any *a priori* assumptions concerning the unmeasured Fourier components, which reduces both noise and truncation effects. At the same time no detailed atomic model is needed for the refinement. The basic input required by the computer code MEND [28] used in the data treatment is the space group, the lattice constants and the flipping ratio's together with the corresponding measured nuclear structure factors. The unit cell of Ba(Fe$_{1-x}$Co$_x$)$_2$As$_2$, $x = 0.066$ was divided into $52 \times 52 \times 52 = 140\,608$ cells, in which the magnetization was assumed to be constant. The reconstruction was started from a flat magnetization distribution with a total moment in the unit cell equal to the bulk magnetization. The result of the reconstruction as compared to the crystal structure of Ba(Fe$_{1-x}$Co$_x$)$_2$As$_2$, $x = 0.066$ is shown in fig. 3. In fig. 3(a) the projection of the density maps and the crystal structure along the tetragonal axis are shown. A projection along the [110] direction is shown in fig. 3(b). As can be seen, these maps exhibit clear, positive density clouds around the Fe/Co positions, whereas the density in the vicinity of the Ba/As positions is quite small.

From fig. 3 it is apparent that the magnetization distribution associated with the Fe/Co sites is not spherical. Interestingly, its shape is different with respect to distribution determined by Brown *et al.* [25] for BaFe$_2$As$_2$ that showed extensions along the [111] directions. In our case, the magnetization distribution is in the form of oblate spheroid with the short axis along the c-axis. If projected
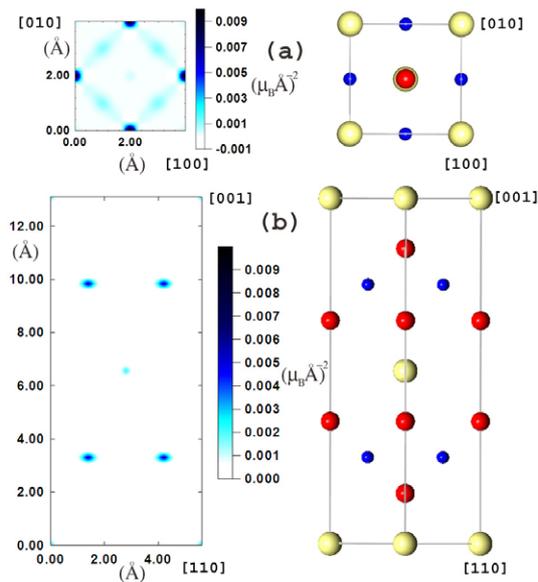
Fig. 3: (Color online) Maximum entropy reconstruction of the magnetization distribution in $Ba(Fe_{1-x}Co_x)_2As_2$, $x = 0.066$ at 25 K with the field applied along the $[\bar{1}10]$ direction projected along the tetragonal axis (a) and along the [110] direction (b) together with relevant projections of the crystal structure. Fe/Co atoms are in blue (small spheres), As in red (intermediate spheres), Ba in yellow (large spheres). All projections are drawn in scale.

along the tetragonal axis, one can detect positive magnetization density bridges along the [110]-type directions connecting the Fe/Co sites.

As one lowers the temperature below the superconducting phase temperature, flipping ratios are getting closer to 1.00 suggesting that the magnetic part is even smaller than at 25 K. This fact, leading to larger error bars, prevented us from analyzing these data and drawing any conclusions regarding the magnetism in superconducting state.

Discussion. – To date we are aware of three attempts to determine the magnetic form factor and magnetization distribution in $AEFe_2As_2$, (AE = Ca, Sr, Ba) iron arsenides, two dealing with $SrFe_2As_2$ [29,30] and remaining for $BaFe_2As_2$ [25] in its tetragonal state. The experimental results in the case of $SrFe_2As_2$ obtained by both groups came to contradictory conclusions. One of the studies suggested extended magnetization clouds along the Fe-As bonds [30] while the other, supported also by calculated magnetic form factors using the first-principles electronic structure method [29], revealed extended densities in the basal plane along the [100] and [110] directions. Some recent studies of the iron arsenides suggest that the orthorhombic structural distortion at T_{TO} is connected with an orbital ordering [31,32]. Due to the anisotropy of the d_{xz} and d_{yz} orbitals in the xy plane, a ferro-orbital ordering makes the orthorhombic structure more energetically favorable, significantly re-populating various orbitals [33]. Other work strongly indicates that

the driving mechanism arises from magnetic fluctuations and magnetic order with any orbital ordering playing a minor role [34]. All these findings make a comparison with the first two studies impossible as they were performed in magnetically ordered and orthorhombic-distorted states. The latter study has been in principle performed under similar conditions. However, even here the agreement is limited. Common to all studies is the fact that the magnetization density is associated with crystallographic sites occupied by Fe or by Fe/Co atoms and, most importantly, that it involves an orbital part. The density in the antiferromagnetically ordered state is high, corresponding to a rather large ordered Fe magnetic moments. The density in the paramagnetic state of $BaFe_2As_2$ or $Ba(Fe_{1-x}Co_x)_2As_2$, $x = 0.066$ is about three orders of magnitude smaller. The study of Brown *et al.* [25] suggests magnetization densities squeezed along the tetragonal axis and extended along the [111] direction. A detailed refinement revealed predominant occupation of the xy-type singlet orbital. Our study suggests also magnetization less extended in the c-axis direction but, in contrary, an elongation mainly along the [110] direction. The former scenario would be in agreement with recent ARPES studies showing strongly orbital-dependent modifications of the electronic structure across the magnetostructural transitions [19]. However, it has to be noted that the magnetization distribution probed by PND arises from redistribution caused by electrons states near the Fermi surface, *i.e.* by electron states that might be different from those responsible for long-range magnetic order that are usually well below the Fermi energy.

Conclusions. – In conclusion, we have determined the magnetic form factors in $Ba(Fe_{1-x}Co_x)_2As_2$, $x = 0.066$ just above the transition to the superconducting state by means of a PND experiment. The magnetic signal induced by magnetic field of 6 T applied along the $[\bar{1}10]$ direction is clearly connected with Fe/Co sites and contains also orbital contributions. Density maps obtained by means of maximum entropy reconstruction are in $Ba(Fe_{1-x}Co_x)_2As_2$, $x = 0.066$ at 25 K different than those reported earlier for $BaFe_2As_2$ at 200 K and for two studies using $SrFe_2As_2$ at low temperatures. This is not surprising for both latter studies, which were performed on AF ordered systems that were orthorhombically distorted in contrast to the tetragonal compound studied here. The remaining study on $BaFe_2As_2$ at high temperature [25], which appeared upon performing the study described here, revealed positive densities in directions connecting Fe and As positions suggesting the hybridization between these two atomic species. Our results indicate the presence of a strong Fe-Fe interaction within the basal plane. Along the tetragonal axis, much weaker extension of the densities were found. Upon entering the SC state, the signal gets even smaller making any type of conclusion regarding the magnetism in the superconducting state difficult.

REFERENCES

[1] Kamihara Y., Hiramatsu H., Hirano M., Kawamura R., Yanagi H., Kamiya T. and Hosono H., *J. Am. Chem. Soc.*, **128** (2006) 10012.

[2] Rotter M., Tegel M. and Johrendt D., *Phys. Rev. Lett.*, **101** (2008) 107006.

[3] Ishida Y., Nakai F. and Hosono H., *J. Phys. Soc. Jpn.*, **78** (2009) 062001.

[4] Canfield P. C., Bud'ko S. L., Ni N., Kreyssig A., Goldman A. I., McQueeney R. J., Torikachvili M. S., Argyriou D. N., Luke G. and Yu W., *Physica C*, **469** (2009) 404.

[5] Cheng P., Shen B., Mu G., Zhu X., Han H., Zheng B. and Wen H., *EPL*, **85** (2009) 67003.

[6] Zhang Y., Wei J., Ou H. W., Zhao J. F., Zhou B., Chen F., Xu M., He C., Wu G., Chen H., Arita M., Shimada K., Namatame H., Taniguchi M., Chen X. H. and Feng D L., *Phys. Rev. Lett.*, **102** (2009) 127003.

[7] Noffsinger J., Giustino F., Louie S. G. and Cohen M. L., *Phys. Rev. Lett.*, **101** (2009) 147003.

[8] Johnston D. C., *Adv. Phys.*, **59** (2010) 803.

[9] Prokeš K., Kreyssig A., Ouladdiaf B., Pratt D. K., Ni N., Bud'ko S. L., Canfield P. C., McQueeney R. J., Argyriou D. N. and Goldman A. I., *Phys. Rev. B*, **81** (2010) 180506(R).

[10] Nandi S., Kim M. G., Kreyssig A., Fernandes R. M., Pratt D. K., Thaler A., Ni N., Bud'ko S. L., Canfield P. C., Schmalian J., McQueeney R. J. and Goldman A. I., *Phys. Rev. Lett.*, **104** (2010) 057006.

[11] Christianson A. D., Lumsden M. D., Nagler S. E., MacDougall G. J., McGuire M. A., Sefat A. S., Jin R., Sales B. C. and Mandrus D., *Phys. Rev. Lett.*, **103** (2009) 087002.

[12] Pratt D. K., Tian W., Kreyssig A., Zarestky J. L., Nandi S., Ni N., Bud'ko S. L., Canfield P. C. and Goldman A. I., *Phys. Rev. Lett.*, **103** (2009) 087001.

[13] Yildirim T., *Phys. Rev. Lett.*, **101** (2008) 057010.

[14] Belashchenko K. D. and Antropov V. P., *Phys. Rev. B*, **78** (2008) 212505.

[15] Singh K. D., *Physica C*, **469** (2009) 418.

[16] Lumsden M. D., Christianson A. D., Parshall D., Stone M. B., Nagler S. E., MacDougall G. J.,

Mook H. A., Lokshin K., Egami T., Abernathy D. L., Goremychkin E. A., Osborn R., McGuire M. A., Sefat A. S., Jin R., Sales B. C. and Mandrus D., *Phys. Rev. Lett.*, **102** (2009) 107005.

[17] Mittal R., Su Y., Rols S., Tegel M., Chaplot S. L., Schober H., Chatterji T., Johrendt D. and Brückel , *Phys. Rev. B*, **78** (2008) 224518.

[18] Liu T. J., Hu J., Qian B., Fobes D., Mao Z. Q, Bao W., Reehuis M., Kimber S. A. J., Prokeš K., Maťaš Argyriou D. N., Hiess A., Rotaru A., Pham H., Spinu L., Qiu Y., Thampy V., Savici A. T., Rodriguez J. A. and Broholm C., *Nat. Mater.*, **9** (2010) 716.

[19] Shimojima T., Ishizaka K., Ishida Y., Katayama N., Ohgushi K., Kiss T., Okawa M., Togashi T., Wang X.-Y., Chen C.-T., Watanabe S., Kadota R., Oguchi T., Chainani A. and Shin S., *Phys. Rev. Lett.*, **104** (2010) 057002.

[20] Fink J., Thirupathaiah S., Ovsyannikov R., Dürr H. A., Follath R., Huang Y., de Jong S., Golden M. S., Yu-Zhong Zhang, Jeschke H. O., Valentí R., Felser C., Dastjani Farahani S., Rotter M. and Johrendt D., *Phys. Rev. B*, **79** (2009) 155118.

[21] Nathans R., Pigott M. T. and Shull C. G., *J. Phys. Chem. Solids*, **6** (1958) 38.

[22] Ni N., Tillman M. E., Yan J.-Q., Kracher A., Hannahs S. T., Bud'ko S.-L. and Canfield P. C., *Phys. Rev. B*, **78** (2008) 214515.

[23] Rossat-Mignod J., in *Methods of Experimental Physics*, edited by Sköld K. and Price D. L., Vol. **23C** (Academic Press, Inc., New York) 1987, p. 1.

[24] Gukasov A., Goujon A., Meuriot J.-L., Person Ch., Exil G. and Koskas G., *Physica B: Cond. Matter*, **397** (2008) 131.

[25] Brown P. J., Chatterji T., Stunault A., Su Y., Xiao Y., Mittal R., Brückel Th., Wolf Th. and Adelmann P., *Phys. Rev. B*, **82** (2010) 024421.

[26] Skilling J. and Gull S. F., in *Maximum Entropy and Bayesian Methods in Inverse Problems*, edited by Ray Smith C. and Grandy W. T. jr. (Reidel, Dordrecht) 1985, p. 83.

[27] Freeman A. J. and Watson R. E., *Acta Crystallogr.*, **14** (1961) 231.

[28] Sakata M., Uno T., Takata M. and Howard C. J., *J. Appl. Crystallogr.*, **26** (1993) 159.

[29] Lee Y., Vaknin D., Li H., Tian W., Zarestky J. L., Ni N., Bud'ko S.-L. and Canfield P. C., *Phys. Rev. B*, **81** (2010) 060406(R).

[30] Ratcliff W., Kienzle P. A., Lynn J. W., Li S., Dai P., Chen G. F. and Wang L. N., *Phys. Rev. B*, **81** (2010) 140502(R).

[31] Chen C.-C., Maciejko J., Sorini A. P., Moritz B., Singh R. R. P. and Devereaux T. P., *Phys. Rev. B*, **82** (2010) 224506(R).

[32] Chu J.-H., Analytis J. G., De Greve K., McMahon P. L., Islam Z., Yamamoto Y. and Fisher I. R., *Science*, **329** (2010) 824.

[33] Lv W., Wu J. and Phillips P., *Phys. Rev. B*, **80** (2009) 224506.

[34] Daghofer W., Luo Q.-L., Yu R., Yao D.-X., Moreo A. and Dagotto E., *Phys. Rev. B*, **81** (2010) 180514(R).